

# Drell-Yan Production of W/Z at the LHC with Protons and Heavy Nuclei

D. BENJAMIN CLARK

*Southern Methodist University  
Dallas, TX 75206, USA*

Drell-Yan W/Z electroweak boson production at the LHC is an essential standard candle which is used for calibration of beam luminosity and detector properties. In addition to proton-proton collisions, the LHC has measured heavy nuclei lead-lead and proton-lead W/Z production. Inclusion of these data sets in future fits can provide discriminating information of the nuclear modifications present in the Parton Distribution Functions (PDFs). We present an ongoing analysis of W/Z production in lead-lead and proton-lead collisions at the LHC using the **nCTEQ15** nuclear Parton Distribution Functions (nPDFs) including uncertainties. The cross sections are calculated at NLO with the **FEWZ 2.1** program at 2.76 and 5.02 TeV. We identify promising observables for the observation of the nuclear modifications.

PRESENTED AT

DPF 2015

The Meeting of the American Physical Society  
Division of Particles and Fields  
Ann Arbor, Michigan, August 4–8, 2015

# 1 Introduction

Parton Distribution Functions (PDFs) are an essential component for the calculation of any observable in hadronic collisions. Collisions involving Heavy Nuclei (HI) require input from nuclear PDFs (nPDFs) which show significant modifications to free proton PDFs. These modifications were first seen by the EMC collaboration in 1983 [1] and later measured and described by SLAC in the 1980s and '90s (e.g. see [2]). The nuclear modifications across the  $x$  range are generally known as shadowing, anti-shadowing, the EMC effect, and Fermi motion.

Recently, the **nCTEQ** collaboration has produced a new set of nPDFs for 19 different values of  $A$  as explained in [3, 4]. These nPDFs can be used to compute observables for HI collisions at NLO along with Hessian estimations of the PDF errors. The nuclear modifications to the free proton PDF are described by an  $A$ -dependent parameterization fit to data from DIS, D-Y, and inclusive pion production. The  $A$ -dependence is given to the parameters of the free proton PDF such that a value of  $A, Z = 1$  will reproduce the free proton.

Hessian error sets are provided for the errors on the nuclear parameters only. These errors are much larger than the errors on the proton PDF parameterization as can be seen in Fig. 1. Therefore errors shown in this note are due to the nuclear parameters only. At this time, no statistically sound method to combine the errors on the free proton parameters with the errors on the nuclear parameters exists in the literature.

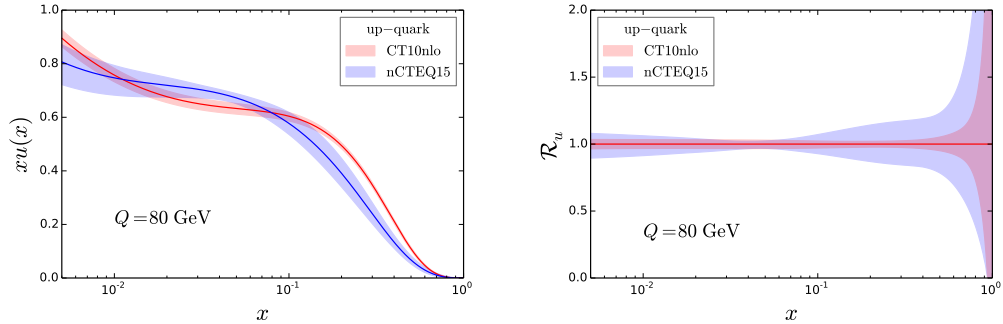


Figure 1: The left plot shows the **nCTEQ15** bound Pb PDF compared to the CT10 free proton. The initial state modifications are apparent in the softening of the valance quark peak. On the right the ratio demonstrates that the free proton PDF is much more tightly constrained over the entire range of  $x$ .

The full nuclear target PDF is constructed from the bound neutron and proton PDFs,  $f_i^{n/A}(x, Q)$  and  $f_i^{p/A}(x, Q)$  respectively as,

$$f_i^{(Q,Z)}(x, Q) = \frac{Z}{A} f_i^{p/A}(x, Q) + \frac{(A-Z)}{A} f_i^{n/A}(x, Q), \quad (1)$$

where  $A - Z$  is the number of neutrons in the nuclear target. In the above equation the bound neutron PDF is found by the approximate isospin symmetry present at NLO. That is, the neutron PDF is constructed by the replacements  $u \longleftrightarrow d$  and  $\bar{u} \longleftrightarrow \bar{d}$  in the proton PDF.

## 2 Vector Boson Production

The LHC produces many electroweak bosons at high rapidity and properties of these bosons have been well-studied [5–12]. In the factorization formalism, the cross section for lepton pair production is written as a convolution of the partonic cross section with the PDFs for each of the colliding hadrons as,

$$\frac{d\sigma}{dQ^2 dy} = \sum_{a,b} \int_0^1 d\xi_1 \int_0^1 d\xi_2 \frac{d\hat{\sigma}^{a,b}}{dQ^2 dy} f_{a/A}(\xi_1) f_{b/B}(\xi_2). \quad (2)$$

The PDFs are integrated over the longitudinal momentum fractions  $\xi_{1,2}$  of the partons involved in the interaction. In the collinear approximation, the longitudinal momentum fraction becomes the Bjorken scaling variable  $x$ . For fixed partonic energy  $Q$ , a change in rapidity,  $y$ , corresponds to a change in the relative fractions of  $x_{1,2}$  for the incoming partons. Thus, measurement of the rapidity distribution of lepton pairs produced in hadronic collisions gives a handle on the PDF distributions in  $x$ .

In addition, comparison of different observables involving electroweak bosons allows for flavor decomposition in the measured PDFs. This is because different quark flavors contribute to the production of different vector bosons. For example, the major contribution to the  $W^+$  cross section is the  $u - \bar{d}$  interaction while the major contribution to the  $W^-$  cross section is the  $d - \bar{u}$  interaction. These two measurements are very sensitive to the  $u$  and  $d$  parameterization in the fits and allow for comparison of the various nPDF releases.

The contribution of the error on each flavor to the overall error on the measurements can be estimated by looking at the cosine of the correlation angle as defined in [13], see Fig. 2. A correlation of  $\approx 1$  indicates that the error on the measurement of this observable is being driven by the error on that quark flavor. Furthermore, a high correlation indicates that the inclusion of this measurement in the fit will directly constrain the error on that quark flavor. The correlation presented here also shows that the  $u$  and  $d$  quark PDFs are anti-correlated over the range of  $x$ . This anti-correlation results in the decomposition of these flavors and helps to constrain their PDFs.

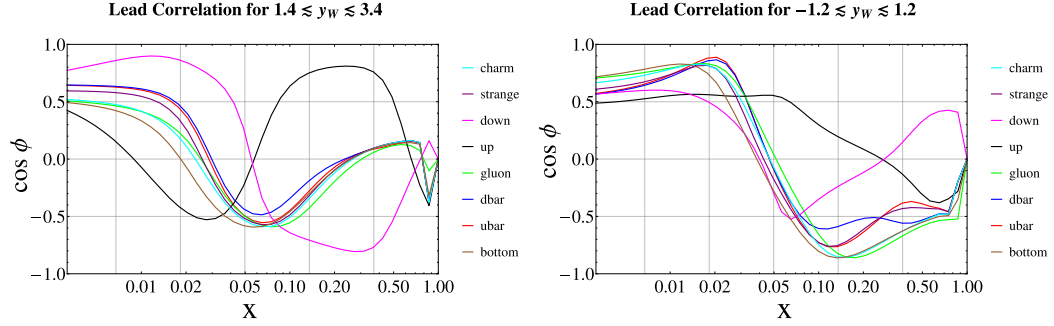


Figure 2: The cosine of the correlation angle for the  $W^+$  cross section for the various flavors as a function of  $x$ . The left plot shows the high rapidity bins and the right plot shows the central region.

### 3 Results

All calculations in this preliminary study have been performed at NLO with FEWZ 2.1 [14] modified to accept two different PDFs for the two interacting nuclei. The code was benchmarked against the original version of FEWZ 2.1 for the pp and PbPb cases and demonstrated exact agreement. All calculations are performed and presented in the center of momentum (COM) frame. The COM frame for PbPb collisions corresponds to the lab frame as the two colliding beams have the same energy. For the pPb collisions the lab frame is shifted relative to the COM frame by  $\eta_{LAB} = \eta_{COM} + 0.465$ . This rapidity shift is not accounted for in this study and will be included when comparing to the available data.

#### 3.1 Lead Lead Collisions

The cross sections for PbPb collisions at 2760 GeV COM energy at the LHC were computed and compared to predictions for a lead nucleus constructed from CT10 free proton PDFs according to Eq. (1). While the effects of the initial state modifications are visible in the cross sections, these effects are washed out by the isoscalarity of the Pb nucleus; that is, the uncertainty bands for the two calculations overlap significantly. This fact coupled with a systematically dominated measurement leaves little hope for detecting the nuclear modifications to electroweak boson production in PbPb collisions at this energy.

#### 3.2 Proton Lead Collisions

The Vector Boson cross section in pPb collisions at 5020 GeV provide a chance to see the nuclear modifications and compare predictions from different nPDF releases. In

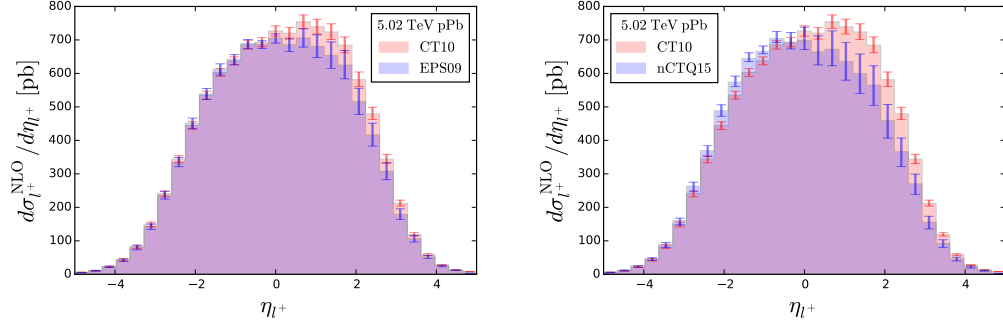


Figure 3: The lepton rapidity distribution for pPb collisions at 5020 GeV at the LHC for EPS09 + CT10 (left) and nCTEQ15 (right) nPDFs compared to the distribution with the lead nucleus constructed from the CT10 free proton PDF. The initial state modifications to the PDF have a dramatic effect on the distribution.

Fig. 3 we see a comparison of the differential cross sections calculated with nCTEQ15, EPS09 + CT10 [15], and CT10 [16] PDFs. These distributions are asymmetric because of different number of nucleons in each of the colliding nuclei.

The shape of the distribution can be understood by considering the LO calculation. In light-cone coordinates, the momentum fraction can be written  $x = \tau e^{\pm y}$  where  $+y$  is the rapidity of the beam with  $x_1$ ,  $-y$  is the rapidity of the beam with  $x_2$ , and  $\tau = Q/\sqrt{S}$ . For 5020 GeV, we have  $\tau \approx 0.016$  for on-shell  $W^\pm$  production. This is equal to the momentum fraction at central rapidity. Moving to positive or negative rapidities is equivalent to a scan in the  $x_1$   $x_2$  plane. That is, as  $y$  increases,  $x_1$  increases and  $x_2$  decreases. Therefore, scanning in  $y$  probes the contributions to the PDF due to the nuclear modifications.

The asymmetry of the pPb cross sections can be anticipated by comparing the free proton PDF to the bound proton PDF in Fig. 1. At LO, the PDF can be thought of as the number density for each quark. At negative rapidities, the momentum fraction  $x_2$  for the bound lead PDF increases and from Fig. 1 we see that we move into an anti-shadowing region where the Pb PDF is increasing and the proton PDF is suppressed. The opposite occurs for positive rapidity. So we expect an enhanced (suppressed) number density in the region where  $y < 0$  ( $y > 0$ ). This corresponds to more (fewer) valance quarks available for the interaction.

The initial state modifications to the nPDFs have the startling effect of shifting the maximum of the cross section from the region of positive rapidity to the region of negative rapidity as seen in Fig. 3. The combination of proton and neutron PDFs in the CT10 calculation enhances the cross section when  $x_1$  is large and  $x_2$  is small.

We also compare the shapes of the distributions from nCTEQ15 and EPS09 + CT10 and find significant differences as seen in Fig. 3. The differences are most pronounced in the high absolute rapidity region where the ratios of  $u(x, Q)/d(x, Q)$

and  $\bar{u}(x, Q)/\bar{d}(x, Q)$  become significant. Note that these ratios are one of the main differences between the various nPDF releases.

## 4 Conclusions

Lepton rapidity distributions for on-shell vector boson production in PbPb and pPb collisions at 2760 and 5020 GeV at the LHC have been computed with **FEWZ 2.1**. The effects of the nuclear modifications to the PDFs are seen in the produced lepton rapidity distributions. In the PbPb case, the cross sections with nuclear modifications are consistent with a construction of the nucleus with free proton PDFs.

Vector Boson production in pPb interactions provide an opportunity to observe the initial state modifications to the cross sections. The asymmetry inherent in the cross sections is heavily modified by the nuclear corrections. Additionally, these observables allow for comparison of different nPDF releases as differences in parameterization between them lead to quantitatively different results.

The inclusion of LHC measurements in future nPDF fits will allow for stronger constraints on the PDF uncertainties.

## References

- [1] **European Muon** Collaboration, J. J. Aubert *et al.*, “The ratio of the nucleon structure functions  $F_2^n$  for iron and deuterium,” *Phys. Lett.* **B123** (1983) 275.
- [2] J. Gomez *et al.*, “Measurement of the A-dependence of deep inelastic electron scattering,” *Phys. Rev.* **D49** (1994) 4348–4372.
- [3] K. Kovarik *et al.*, “nCTEQ15 - Global analysis of nuclear parton distributions with uncertainties in the CTEQ framework,” [arXiv:1509.00792 \[hep-ph\]](#).
- [4] I. Schienbein, J. Y. Yu, K. Kovarik, C. Keppel, J. G. Morfin, F. Olness, and J. F. Owens, “PDF Nuclear Corrections for Charged and Neutral Current Processes,” *Phys. Rev.* **D80** (2009) 094004, [arXiv:0907.2357 \[hep-ph\]](#).
- [5] **CMS** Collaboration, S. Chatrchyan *et al.*, “Study of Z production in PbPb and pp collisions at  $\sqrt{s_{NN}} = 2.76$  TeV in the dimuon and dielectron decay channels,” *JHEP* **03** (2015) 022, [arXiv:1410.4825 \[nucl-ex\]](#).
- [6] **LHCb** Collaboration, R. Aaij *et al.*, “Observation of Z production in proton-lead collisions at LHCb,” *JHEP* **09** (2014) 030, [arXiv:1406.2885 \[hep-ex\]](#).

- [7] **CMS** Collaboration, V. Khachatryan *et al.*, “Study of  $W$  boson production in pPb collisions at  $\sqrt{s_{NN}} = 5.02$  TeV,” *Phys. Lett. B* **750** (2015) 565–586, [arXiv:1503.05825 \[nucl-ex\]](#).
- [8] **ATLAS** Collaboration, G. Aad *et al.*, “Measurement of  $Z$  boson Production in Pb+Pb Collisions at  $\sqrt{s_{NN}} = 2.76$  TeV with the ATLAS Detector,” *Phys. Rev. Lett.* **110** no. 2, (2013) 022301, [arXiv:1210.6486 \[hep-ex\]](#).
- [9] **ATLAS** Collaboration, G. Aad *et al.*, “Measurement of the production and lepton charge asymmetry of  $W$  bosons in Pb+Pb collisions at  $\sqrt{s_{NN}} = 2.76$  TeV with the ATLAS detector,” *Eur. Phys. J. C* **75** no. 1, (2015) 23, [arXiv:1408.4674 \[hep-ex\]](#).
- [10] **CMS** Collaboration, S. Chatrchyan *et al.*, “Study of  $W$  boson production in PbPb and  $pp$  collisions at  $\sqrt{s_{NN}} = 2.76$  TeV,” *Phys. Lett. B* **715** (2013) 66–87, [arXiv:1205.6334 \[nucl-ex\]](#).
- [11] **ATLAS** Collaboration, G. Aad *et al.*, “Measurement of the  $W \rightarrow \ell\nu$  and  $Z/\gamma^* \rightarrow \ell\ell$  production cross sections in proton-proton collisions at  $\sqrt{s} = 7$  TeV with the ATLAS detector,” *JHEP* **12** (2010) 060, [arXiv:1010.2130 \[hep-ex\]](#).
- [12] **ATLAS** Collaboration, G. Aad *et al.*, “ $Z$  boson production in  $p$ +Pb collisions at  $\sqrt{s_{NN}} = 5.02$  TeV measured with the ATLAS detector,” [arXiv:1507.06232 \[hep-ex\]](#).
- [13] P. M. Nadolsky, H.-L. Lai, Q.-H. Cao, J. Huston, J. Pumplin, D. Stump, W.-K. Tung, and C. P. Yuan, “Implications of CTEQ global analysis for collider observables,” *Phys. Rev. D* **78** (2008) 013004, [arXiv:0802.0007 \[hep-ph\]](#).
- [14] R. Gavin, Y. Li, F. Petriello, and S. Quackenbush, “ $W$  Physics at the LHC with FEWZ 2.1,” *Comput. Phys. Commun.* **184** (2013) 208–214, [arXiv:1201.5896 \[hep-ph\]](#).
- [15] K. J. Eskola, H. Paukkunen, and C. A. Salgado, “EPS09: A New Generation of NLO and LO Nuclear Parton Distribution Functions,” *JHEP* **04** (2009) 065, [arXiv:0902.4154 \[hep-ph\]](#).
- [16] H.-L. Lai, M. Guzzi, J. Huston, Z. Li, P. M. Nadolsky, J. Pumplin, and C. P. Yuan, “New parton distributions for collider physics,” *Phys. Rev. D* **82** (2010) 074024, [arXiv:1007.2241 \[hep-ph\]](#).